

Developing iron nitrosyl complexes as NO donor prodrugs†‡

Sandra A. T. Dillinger, Helmut W. Schmalle, Thomas Fox and Heinz Berke*

Received 15th February 2007, Accepted 11th June 2007

First published as an Advance Article on the web 17th July 2007

DOI: 10.1039/b702461d

A novel class of water-soluble iron nitrosyl complexes has been developed for use as NO donor prodrugs. To elaborate these NO prodrugs various water-soluble ligands were used such as $\text{P}(\text{CH}_2\text{OH})_3$, 1,3,5-triaza-7-phosphatricyclo[3.3.1.1]decane (PTA), 1,2-bis[bis(hydroxymethyl)phosphino]ethane (HMPE), 1,2-bis[bis(hydroxymethyl)phosphino]benzene (TMBz), cysteamine, cysteamine hydrochloride, L-cysteine ethyl ester hydrochloride (LCEE) and pyrimidine-2-thiol (pyrim). The mononuclear complexes $\text{Fe}(\text{NO})_2\text{P}(\text{CH}_2\text{OH})_3\text{Cl}$ **1**, $\text{Fe}(\text{NO})_2(\text{P}(\text{CH}_2\text{OH})_3)_2$ **2**, $\text{Fe}(\text{NO})_2(\text{PTA})_2$ **3**, $\text{Fe}(\text{NO})_2\text{HMPE}$ **4**, $\text{Fe}(\text{NO})_2\text{TMBz}$ **5**, $[\text{Fe}(\text{NO})_2\text{pyrim}]$ **10**, $[\text{Fe}(\text{NO})_3\text{P}(\text{CH}_2\text{OH})_3][\text{X}]$ ($\text{X} = \text{PF}_6, \text{SbF}_6, \text{BF}_4$) **11–13** and the dinuclear species $[\text{Fe}(\text{NO})_2\text{S}(\text{CH}_2)_2\text{NH}_3\text{Cl}]_2$ **6a**, $[\text{Fe}(\text{NO})_2\text{S}(\text{CH}_2)_2\text{NH}_3\text{I}_2]$ **6b**, $[\text{Fe}(\text{NO})_2\text{LCEE}]_2$ **8** and $[\text{Fe}(\text{NO})_2\text{pyrim}]_2$ **9** were obtained. Complexes **1**, **2**, **4**, **6a**, **6b**, **11**, **12** and **13** are water-soluble. **1**, **2** and **4** were identified as nitroxyl and **6a**, **6b**, **11**, **12** and **13** as nitric oxide donors by applying an EPR NO-trap assay. To determine the amount of nitric oxide which was released from the nitric oxide donors, an additional electrochemical methodology was used. The equilibrium release or the trapping concentration of NO was also studied by a UV-vis method, which allowed the rate constant of NO release to be determined.

Twenty years ago, NO was discovered to be involved in several physiological and pathophysiological processes in mammals.^{1,2} A lack of NO production has been related to diseases such as hypertension or arteriosclerosis. In such cases organic and metal organic NO prodrugs, which under physiological conditions release nitric oxide, have been widely used in clinical treatments. The most important of which are the triglyceryl³ and the sodium nitroprusside (SNP) compounds.⁴ Meanwhile major problems such as nitrate tolerance for triglyceryl and cyanide poisoning for SNP have been revealed for some patients.⁵ In this paper we present the synthesis of new nitroxyl and nitric oxide donors and their analysis by biophysical methods such as electron paramagnetic resonance^{2,6} (EPR-NO trap method) and electrochemistry. These methods not only allowed us to detect and identify⁷ the nature of the released NO, but also to quantify⁸ the amount of NO generated under pseudo-physiological conditions. In such a way, kinetic studies using pseudo-first order conditions have also been carried out to determine the rate constant of NO release.

Results and discussion

The paramagnetic d^7 $\text{Fe}(\text{NO})_2\text{P}(\text{CH}_2\text{OH})_3\text{Cl}$ **1** is a $17e^-$ complex,⁹ which can be prepared by the reaction of $[\text{Fe}(\text{NO})_2\text{Cl}]_2$ ¹⁰ with two equivalents of $\text{P}(\text{CH}_2\text{OH})_3$ ¹¹ at r.t. Compound **1** is a rose powder with high solubility and stability in water and alcohols. It crystallizes with varying amounts of solvent so that correct

elemental analysis could not be obtained. The ³¹P NMR spectrum shows one singlet at around $\delta = 59.5$ ppm corresponding to a metal bound phosphine.¹¹ In the IR spectrum of **1** the NO bands are found at 1720 and 1678 cm^{-1} . They are shifted to lower frequencies as compared to the dinuclear starting material where the bands are found at 1810 and 1725 cm^{-1} . Conductivity measurements showed that **1** behaves in water as a 1 : 1 electrolyte. Here the chloro ligand seems to ionise off, as demonstrated in Fig. 1.

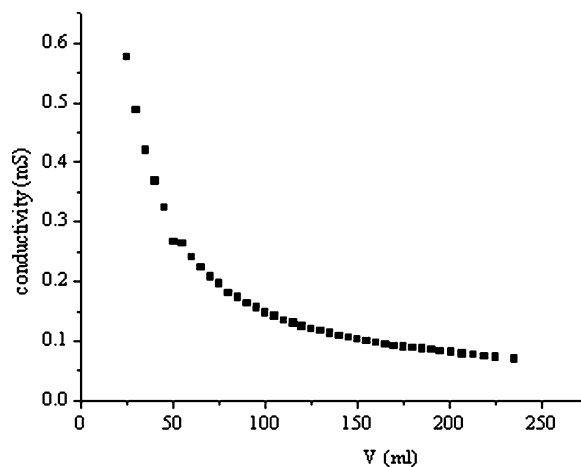


Fig. 1 Conductivity of a dilution series of $\text{Fe}(\text{NO})_2\text{P}(\text{CH}_2\text{OH})_3\text{Cl}$ in water at 25 °C. Conductivity $A_m = 195.56 \text{ S cm}^2 \text{ mol}^{-1}$.

The diamagnetic d^6 complex $\text{Fe}(\text{NO})_2[\text{P}(\text{CH}_2\text{OH})_3]_2$ ¹² **2** can be obtained from the reaction between $\text{Fe}(\text{CO})_2(\text{NO})_3$ ¹³ and two equivalents of $\text{P}(\text{CH}_2\text{OH})_3$. Complex **2** is a red solid and possesses good solubility and stability in polar solvents such as water, alcohols and THF. The ³¹P NMR spectrum displays one singlet at $\delta = 52.1$ ppm corresponding to the two chemically equivalent phosphorus nuclei. The ¹³C NMR spectrum shows one multiplet

Anorganisch-chemisches Institut, Universität Zürich, Winterthurerstrasse 190, 8057, Zürich, Switzerland. E-mail: hberke@aci.unizh.ch.; Fax: +41 44 635 68 02; Tel: +41 44 635 46 81

† CCDC reference numbers 610298–610305. For crystallographic data in CIF or other electronic format see DOI: 10.1039/b702461d

‡ Electronic supplementary information (ESI) available: Complete structural plot of compound **6b** and the calibration curve of the ISO NO electrode. See DOI: 10.1039/b702461d

at 59.3 ppm that corresponds to an AA'XX' spin system and is assigned to the CH₂ groups. Furthermore the two nitrosyl bands shift from 1810 and 1756 cm⁻¹ for Fe(CO)₂(NO)₂ to 1711 and 1668 cm⁻¹ for **2**. Such lower values of ν(NO) bands are in accordance with data for related complexes bearing two phosphine ligands.¹⁴ **2** was recrystallized from water to obtain crystals suitable for an X-ray diffraction study¹⁵ (Fig. 2).

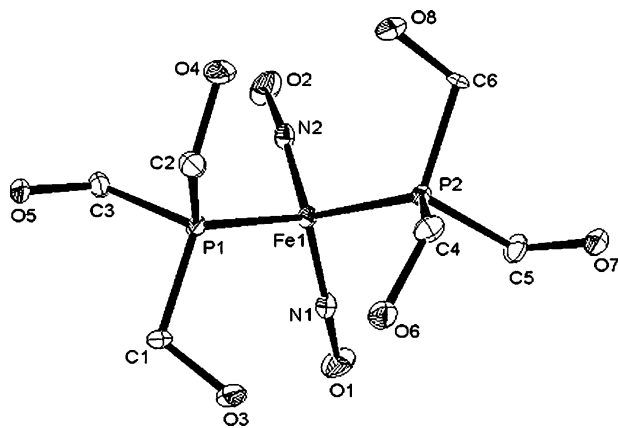


Fig. 2 Molecular structure of Fe(NO)₂(P(CH₂OH)₃)₂ **2** (showing 30% probability displacement ellipsoids). Hydrogen atoms have been omitted for clarity.

The diamagnetic d⁶ Fe(NO)₂(PTA)₂ compound **3** (PTA = 1,3,5-triaza-7-phosphatricyclo[3.3.1.1]decane) can be prepared from Fe(NO)₂(CO)₂ with two equivalents of PTA.¹⁶ **3** is a red solid and is slightly water-soluble, but highly soluble in polar organic solvents. The ³¹P NMR spectrum shows one singlet at δ = -25.5 ppm corresponding to two chemically equivalent phosphorus atoms. In the IR spectrum of **3** we again observe a shift of the NO bands to lower frequencies (1715, 1668 cm⁻¹) in comparison with the starting material Fe(CO)₂(NO)₂. **3** cocrystallized with THF giving crystals suitable for an X-ray diffraction study¹⁷ (Fig. 3). Compound **3** exhibits twofold symmetry with the Fe atom on a

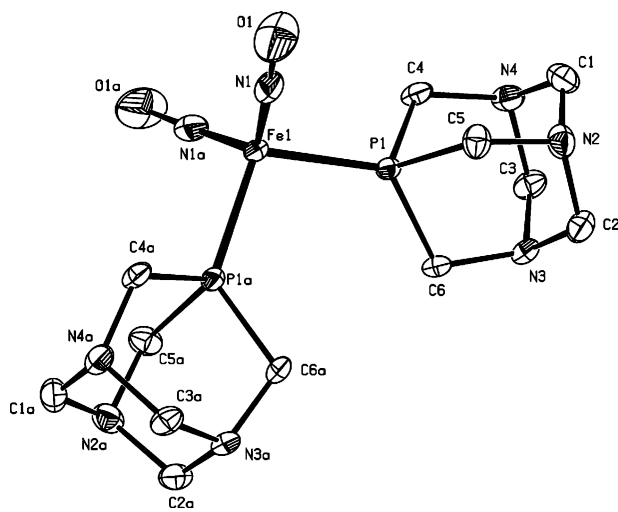


Fig. 3 Molecular structure of Fe(NO)₂(PTA)₂ **3** (showing 50% probability displacement ellipsoids). Hydrogen atoms have been omitted for clarity. Atoms at the left-hand side with an "a" added to the labels are at equivalent positions (1 - x, y, ½ - z).

crystallographic twofold axis. The THF solvate molecule lies on a center of inversion (1.5 - x, 1.5 - y, -z) and was refined with nine distance restraints.

The diamagnetic d⁶ compound Fe(NO)₂HMPE **4** (HMPE = 1,2-bis[bis(hydroxymethyl)phosphino]ethane) was obtained from the reaction between Fe(CO)₂(NO)₂ and one equivalent of HMPE.^{17,18} **4** is a red solid with higher solubility in water than **2** and **3**. As for the previous complexes the nitrosyl bands are shifted in the IR spectrum to lower frequencies (1711, 1664 cm⁻¹). **4** could be recrystallized from water allowing isolation of crystals suitable for an X-ray diffraction study, which proved that the bisphosphine HMPE binds to the metal center in a bidentate fashion (Fig. 4).

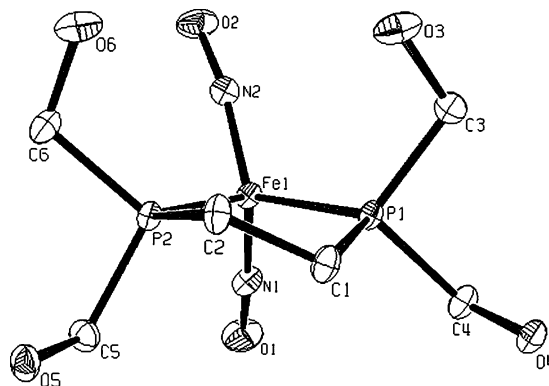


Fig. 4 Molecular structure of Fe(NO)₂HMPE **4** (showing 30% probability displacement ellipsoids). Hydrogen atoms have been omitted for clarity.

Another bisphosphine which was explored to function as a water-soluble ligand in iron dinitrosyl complexes, was 1,2-bis[bis(hydroxymethyl)phosphino]benzene (TMBz). This bisphosphine has similar water-solubility and air stability as HMPE. TMBz reacts with the dicarbonyl dinitrosyl iron compound to afford the substitution product **5** in a relatively low yield of 20%. As in compound **4** the TMBz ligand is assumed to bind to the metal center in a bidentate fashion. In contrast to HMPE, **5** was not water-soluble and crystals suitable for an X-ray diffraction study could not be isolated.

The ionic d⁷ dinuclear species [Fe(NO)₂·S(CH₂)₂NH₃]₂Cl₂ **6a** and [Fe(NO)₂·S(CH₂)₂NH₃]₂I₂ **6b** were EPR silent, which pointed to strong antiferromagnetically coupled iron centers.¹⁹ **6a** can be obtained in THF by the reaction of Fe(CO)₂(NO)₂ with one equivalent of cysteamine hydrochloride.²⁰ **6a** is an ochre solid and highly soluble in water. The IR spectrum of **6** exhibits NO bands at 1794 and 1753 cm⁻¹, whereas a band for a N-H vibration is found at 1468 cm⁻¹ corresponding in its position to an ammonium derivative. Recrystallization of **6a** gave crystals suitable for an X-ray diffraction study (see ESI†). Its structure is similar to that of compound **6b**. The iron-iron contact Fe(1)-Fe(1)#1 amounts to 2.7154(11) Å and is characteristic for a ligand supported metal-metal single bond.¹⁹

Species [Fe(NO)₂·S(CH₂)₂NH₃]₂I₂ **6b** could be prepared in THF by the reaction of the dinuclear complex [Fe(NO)₂]₂²¹ with two equivalents of the cysteamine ligand. **6b** is a brown solid and highly soluble in water. The IR spectrum shows a shift of the NO bands to lower frequencies (1782 and 1751 cm⁻¹), and the ν(NH) band of the non-coordinated ammonium unit is found at 1464 cm⁻¹. **6b** could be recrystallized from water to obtain crystals suitable for an

X-ray diffraction study (Fig. 5). The Fe(1)–Fe(1)#1 (2.7075(10) Å) bond length is very similar to that of **6a** and again corresponds to an iron–iron single bond.¹⁹

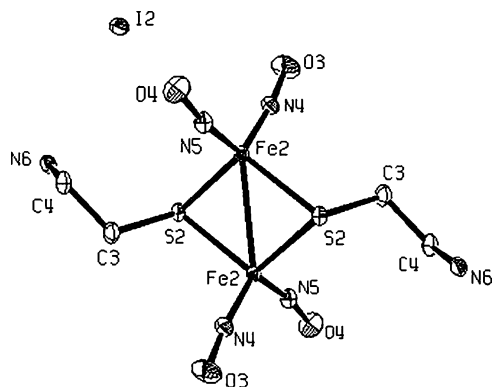


Fig. 5 Molecular structure of $\text{Fe}(\text{NO})_2\text{S}(\text{CH}_2)_2\text{NH}_2]_2$ **6b** (showing 50% probability displacement ellipsoids). Hydrogen atoms have been omitted for clarity. One water solvate molecule (not shown) completes the structure. The complete structure of **6b** is given in the ESI† (Fig. 5).

Complexes containing amino acid ligands could only be obtained with L-cysteine ethyl ester hydrochloride. It was not possible to substitute CO groups in $\text{Fe}(\text{NO})_2(\text{CO})_2$ with glycine or cysteine or induce related reactions with the $[\text{Fe}(\text{NO})_2\text{X}]_2$ complexes ($\text{X} = \text{Cl}, \text{I}$). One equivalent of ethyl L-cysteine hydrochloride was thus reacted with $\text{Fe}(\text{CO})_2(\text{NO})_2$ in THF at r.t. giving **8** in a yield of 50%. **8** is only slightly water-soluble. Crystals suitable for an X-ray diffraction study could not be obtained, because **8** decomposed in organic solvent after a few days.

The dinuclear $[\text{Fe}(\text{NO})_2\text{pyrim}]_2$ **9** (pyrim = pyrimidine-2-thiol) compound is obtained by mixing $\text{Fe}(\text{CO})_2(\text{NO})_2$ in THF with one equivalent of the ligand pyrimidine-2-thiol.²² **9** is a black solid which is insoluble in water, but highly soluble in polar organic solvents. The IR spectrum exhibits two NO bands at 1794 and 1759 cm^{-1} , which are shifted to lower frequencies in comparison with $\text{Fe}(\text{CO})_2(\text{NO})_2$. **9** was recrystallized from THF–ether to obtain crystals suitable for an X-ray diffraction study (Fig. 6). **9** is structurally related to **6a, b** showing an iron–iron bond distance of 2.7242(10) Å. As in **6a, b** there is strong antiferromagnetic coupling of the iron centers.

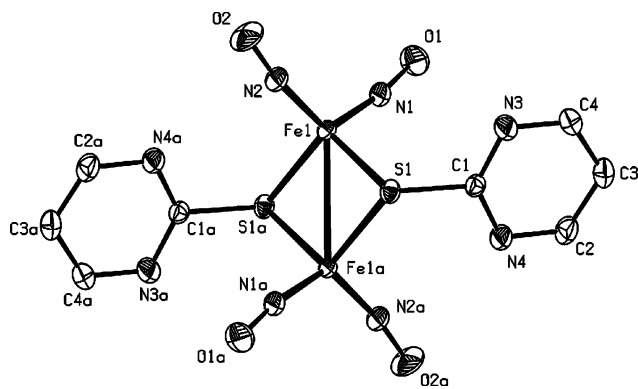


Fig. 6 Molecular structure of $[\text{Fe}(\text{NO})_2\text{pyrim}]_2$ **9** (showing 50% probability displacement ellipsoids). Hydrogen atoms have been omitted for clarity. Atoms labelled “a” denote inversion symmetry ($-x, -y, -z + 1$).

The paramagnetic mononuclear $[\text{Fe}(\text{NO})_2(\text{pyrim})\text{I}]$ complex **10** is obtained by splitting of $[\text{Fe}(\text{NO})_2\text{I}]_2$ with two equivalents of pyrimidine-2-thiol. **10** is a black solid which is insoluble in water, but highly soluble in polar organic solvents. The IR spectrum exhibits two NO bands at 1790 and 1722 cm^{-1} . **10** can be recrystallized from THF–ether to give suitable crystals for a X-ray diffraction study²³ (Fig. 7). The protonation of atom S1 could be verified by difference electron density calculations. Protonation at N3 and N4 was not observed.

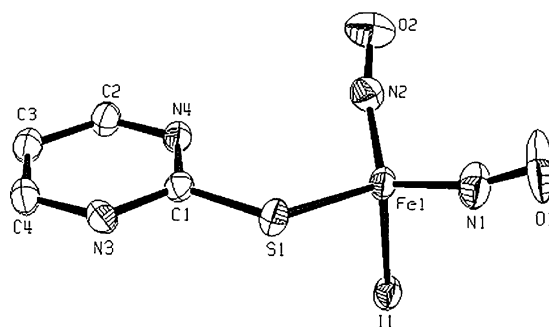


Fig. 7 Molecular structure of $[\text{Fe}(\text{NO})_2\text{pyrim}]\text{I}$ **10** (showing 50% probability displacement ellipsoids). Hydrogen atoms have been omitted for clarity.

In 1978 the first trinitrosyl iron compounds containing trimethylphosphine and triphenylphosphine were synthesized by M. Herberhold *et al.*²⁴ These complexes are cationic nitrosyl metal systems and readily release NO at r.t. We prepared the trinitrosyl complexes **11**, **12** and **13** possessing PF_6^- , BF_4^- and SbF_6^- counter ions. These compounds were obtained *via* the reaction of dicarbonyldinitrosyl iron and various nitrosyl salts²⁵ (NOPF_6 , NOBF_4 and NOSbF_6) in the presence of one equivalent of the water-soluble $\text{P}(\text{CH}_2\text{OH})_3$ ligand. **11**, **12** and **13** are deep green solids highly soluble in water and polar organic solvents. In the IR spectrum the $\nu(\text{NO})$ bands are found at 1925 and 1832 cm^{-1} . They are shifted to higher frequencies in comparison to the $\text{Fe}(\text{CO})_2(\text{NO})_2$ complex. **11** could be recrystallized from CH_3NO_2 –toluene to afford tiny crystals, which were still suitable for an X-ray diffraction study. Due to the small size and irregular shape of the crystal an absorption correction could not be carried out. A split position has been observed for one OH group of the $\text{P}(\text{CH}_2\text{OH})_3$ ligand (Fig. 8). This is the first crystal structure of such a trinitrosyl iron complex.

Detection and identification of NO release: the EPR NO-trap method

The EPR NO-trap assay has been widely used in the biomedical area to detect the release of small amounts of NO *in vitro*. Additionally in 2000, Y. Xia *et al.* published a method to identify the oxidation state of any NO species in water.²⁶ They demonstrated that a $\text{Fe}(\text{MGD})_2$ (*N*-methyl-D-glucamine dithiocarbamate iron) can act as a NO trap and allows discrimination of NO from NO^- (nitroxonium) release depending on the redox state of the $\text{Fe}(\text{MGD})_2$ complex used. $\text{Fe}(\text{II})(\text{MGD})_2$ reacts selectively with NO to give the paramagnetic $(\text{NO})\text{Fe}(\text{II})(\text{MGD})_2$ complex, while the $\text{Fe}(\text{III})(\text{MGD})_2$ species reacts only with NO^- to form the same paramagnetic complex. The $\text{Fe}(\text{MGD})_2$ mononitrosyl complex gives rise to a characteristic three line EPR spectrum.

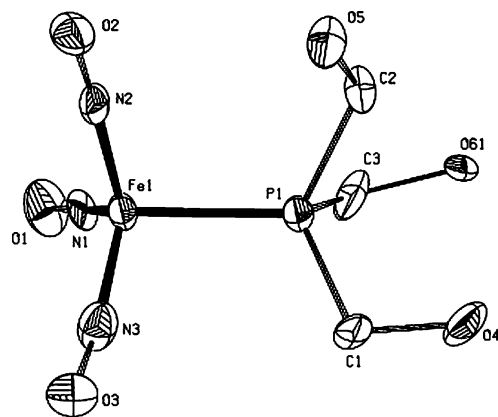


Fig. 8 Molecular structure of $[\text{Fe}(\text{NO})_3\text{P}(\text{CH}_2\text{OH})_3]\text{PF}_6$ **11** showing 10% probability displacement ellipsoids. Hydrogen atoms have been omitted for clarity. One (CH_2OH) group was found to be disordered.

Table 1 Detection of nitroxyl release from compounds **1**, **2** and **4**^a by EPR spectroscopy

NO ⁻ donors	Fe(II)(MGD) ₂	Fe(III)(MGD) ₂
Fe(NO) ₂ P(CH ₂ OH) ₃ Cl 1	—	Three line
Fe(NO) ₂ (P(CH ₂ OH) ₃) ₂ 2	—	Three line
Fe(NO) ₂ HMPE 4	—	Three line

^a Solvent = water, $T = 245\text{--}255$ K.

We systematically carried out two measurements with each of the water-soluble complexes. The Fe(II)(MGD)₂ and Fe(III)(MGD)₂ traps were prepared according to literature procedures.²⁷ The EPR measurements were carried out in frozen water at 245–255 K.

Fe(NO)₂P(CH₂OH)₃Cl **1**, Fe(NO)₂(P(CH₂OH)₃)₂ **2**, and Fe(NO)₂HMPE **4** complexes have thus been identified as nitroxyl donors (Table 1). A three line spectrum was observed only for the ferric form of the trap, which corresponded to the paramagnetic (NO)Fe(I)(MGD)₂ species. The signal possesses a g factor of around 2.05, a center field of 3300 G and a hyperfine coupling constant $a_N = 12.5$ G (Fig. 9).

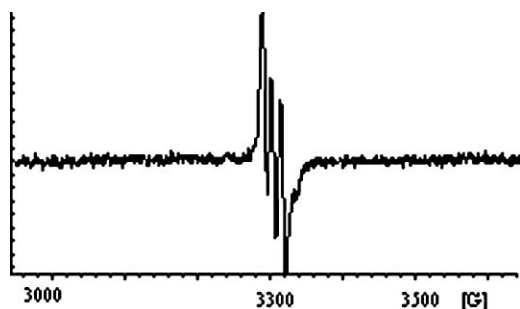


Fig. 9 Three-line spectrum of the (NO)–Fe(III)–(MGD)₂ species at 245–255 K with 50.10^{-4} M Fe(III)(MGD)₂ and 10^{-4} M–NO donors.

On the other hand, the $[\text{Fe}(\text{NO})_3\text{P}(\text{CH}_2\text{OH})_3][\text{X}]$ compounds ($\text{X} = \text{PF}_6$ **11**, BF_4 **12**, SbF_6 **13**), the $[\text{Fe}(\text{NO})_2\text{SCH}_2\text{CH}_2\text{NH}_3]_2\text{Cl}_2$ **6a** and the $[\text{Fe}(\text{NO})_2\text{SCH}_2\text{CH}_2\text{NH}_3]_2\text{I}_2$ **6b** species have been identified as nitric oxide donors (Table 2). Again for each complex, measurements with Fe(III)(MGD)₂ and Fe(II)(MGD)₂ were carried out.

Table 2 Detection of nitric oxide release from compounds **11**, **12**, **13**, **6a** and **6b**^a by EPR spectroscopy

NO ⁻ donors	Fe(II)(MGD) ₂	Fe(III)(MGD) ₂ ^b
$[\text{Fe}(\text{NO})_3\text{P}(\text{CH}_2\text{OH})_3]\text{PF}_6$ 11	Three line	Three line
$[\text{Fe}(\text{NO})_3\text{P}(\text{CH}_2\text{OH})_3]\text{BF}_4$ 12	Three line	Three line
$[\text{Fe}(\text{NO})_3\text{P}(\text{CH}_2\text{OH})_3]\text{SbF}_6$ 13	Three line	Three line
$[\text{Fe}(\text{NO})_2\text{S}(\text{CH}_2)_2\text{NH}_3]_2\text{Cl}_2$ 6a	Three line	Three line
$[\text{Fe}(\text{NO})_2\text{S}(\text{CH}_2)_2\text{NH}_3]_2\text{I}_2$ 6b	Three line	Three line

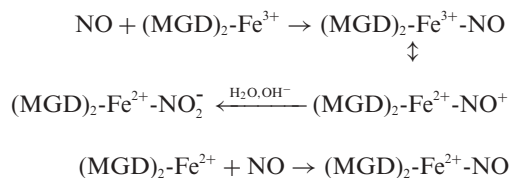
^a Solvent = water, $T = 245\text{--}255$ K. ^b Approximately half of the intensity of Fe(II)(MGD)₂.

Here both traps revealed a three line spectrum corresponding to (NO)Fe(I)(MGD)₂.²⁶

The difference between each of these pairs of spectra lies in the intensity of the signal. For the ferric trap the intensity of the signal is around 40–50% of the ferrous one.

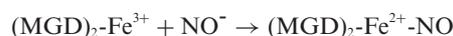
Upon coordination of the nitric oxide (NO) or nitroxyl (NO⁻) ligands to the Fe(II)–(MGD)₂ or the Fe(III)–(MGD)₂ complexes, it is in both cases the $^+\text{ON}\text{--Fe(I)–(MGD)}_2 \leftrightarrow \text{NO}\text{--Fe(II)–(MGD)}_2$ species that are observed by EPR. The mechanism of NO trapping by the Fe(III)–(MGD)₂ complex (reductive nitrosylation) is shown below.

First step: reduction of the Fe³⁺–MGD to the Fe²⁺–MGD species. Second step: trapping of NO by the Fe²⁺–MGD molecule.



NO may also directly react with the Fe(II)–(MGD)₂ trap.

Whereas the nitroxyl molecule (NO⁻) reacts with Fe(III)–(MGD)₂ as shown below:



These results are in accord with those obtained by Y. Xia *et al.*^{26,28} One equivalent of NO is necessary to reduce the Fe(III)(MGD) complexes to the Fe(II)(MGD) whereas the second equivalent of NO released reacts with the ferrous trap to give the paramagnetic (NO)Fe(I)(MGD)₂ species.

Quantification of nitric oxide (NO) release by applying the electrochemical method

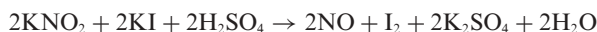
The electrochemical method for nitric oxide quantification offers several possibilities that are not available with spectroscopic approaches. Perhaps the most important is the capability of microelectrodes to directly sense NO in single cells *in situ* in close proximity to the NO source. Electrochemical methods currently available for NO detection are based on the electrochemical oxidation of NO on solid electrodes.²⁹ If the current generated during this oxidation is linearly proportional to the concentration, the anodic current can be taken as an analytical signal. The calibration of the ISO-NO electrode is carried out with the chemical generation of NO and is described elsewhere.³⁰ Once the

sensor has been calibrated direct measurements of the NO released from the NO-donors is possible at the calibration temperature.

Results. To carry out electrochemical NO measurements we used an ISO-NOP 2.0 mm sensor. This electrode is available from World Precision Instruments, USA. It was applied in the amperometric mode with a permanent potential of 865 mV.

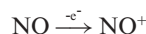
It was necessary to determine a calibration curve at the temperature at which the measurements were to be carried out before any electrochemical NO assay with the NO prodrug was analysed. The calibration of the ISO-NO electrode takes place with chemical generation of NO. It utilises the reaction between a stock solution of a known concentration of sulfuric acid and potassium iodide (0.01 M) and a stock solution of a NO-donor, like sodium nitrite (50×10^{-7} M).

The method of calibration is based on the following reaction:



Since a known amount of KNO_2 is added to produce a known amount of NO, the quantity (and so the concentration) of NO generated can be calculated directly from the stoichiometry, if the concentration of the reactants are known. The potassium iodide and sulfuric acid are present in great excess, potassium nitrite is the limiting reagent generating NO for a period sufficient to calibrate the ISO-NO sensor. Once the sensor has been calibrated, direct measurements of NO from the NO-donors can be carried out.

Generally, the oxidation of NO on solid electrodes proceeds with an "EC mechanism": electrochemical reaction followed by a chemical reaction.² The first electrochemical step is a one-electron transfer from the NO molecule to the electrode resulting in the formation of a nitrosyl cation:



NO^+ is a relatively strong Lewis acid, and in the presence of OH^- it is converted to the nitrite anion (NO_2^-):



The calibration curve can be found in the ESI†.

Firstly, electrochemical measurements were carried out with nitric oxide donors that have been identified by the EPR-trap method *i.e.* the series of the trinitrosyl species **11**, **12**, and **13** and the sulfur containing complexes **6a** and **6b**.

For the trinitrosyl series the electrochemical quantification of the NO release had to be carried out at room temperature, because of high instability of the compounds at elevated temperature, whereas for the compounds **6a** and **6b** the measurements were carried out at 37° C. The results are shown in Tables 3 and 4.

Table 3 Amount of NO released in water determined by electrochemical methods^a

Compound	Amount of NO/mM	Lifetime/s
11	2×10^{-3}	75
12	7.57×10^{-3}	50
13	1.53×10^{-2}	150

^a Experiments were carried out at r.t. for compound **11** (0.086 mM), **12** (0.17 mM), **13** (0.45 mM).

Table 4 Amount of NO released in water determined by electrochemistry^a

Compound	Amount of NO/mM	Lifetime/s
6a	1.49×10^{-5} (zone A)	200
	1.37×10^{-5} (zone B)	—
	1.21×10^{-5} (zone C)	—
6b	0.87×10^{-5} (zone A)	200
	1.62×10^{-5} (zone B)	—
	0.63×10^{-5} (zone C)	—

^a Experiments were carried out at 37° C for compounds **6a** (2.59 mM) and **6b** (1.09 mM).

When compounds **11**, **12** and **13** were dissolved in water, typical oxidation curves were detected (Fig. 10). Single oxidation peaks observed due to the release of only one NO or all NO molecules simultaneously from these compounds during their decomposition in water. The short lifetime, between 50–150 s, of these NO donors mirror their low thermal stability in water.

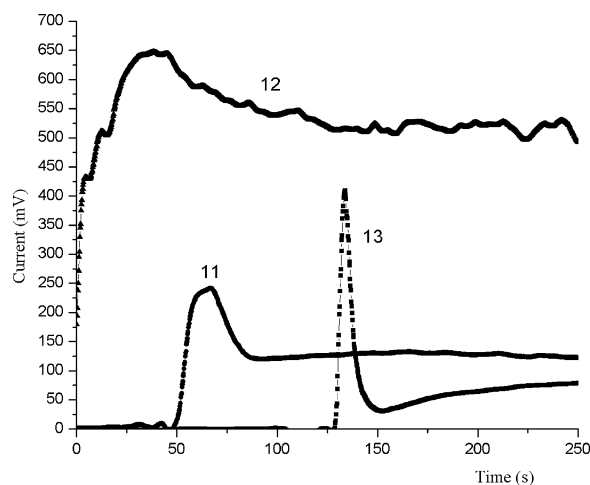


Fig. 10 Decomposition curve of compounds $[\text{Fe}(\text{NO})_3\text{P}(\text{CH}_2\text{OH})_3]\text{PF}_6$ **11**, $[\text{Fe}(\text{NO})_3\text{P}(\text{CH}_2\text{OH})_3]\text{BF}_4$ **12** and $[\text{Fe}(\text{NO})_3\text{P}(\text{CH}_2\text{OH})_3]\text{SbF}_6$ **13** in water at r.t.

Dissolution of compound **6a** and **6b** in water at 37° C leads to rapid decomposition of the latter accompanied by the release of NO (Fig. 11 and 12). At least three oxidation steps are observed here for each complex, which have been designated by zones A, B and C. From Fig. 11 and 12 we can conclude that the lifetime of the dinuclear species **6a** and **6b** is around 200 s.

Another main difference between the two classes of complexes is the mode of NO release. According to the shape of the curves it can be rationalized that the trinitrosyl complexes are able to release either only one or all NO molecules at once, whereas the dinuclear species **6a** and **6b** are able to release NO in a stepwise fashion and practically all of the nitric oxide molecules present in the complex.

We have noticed that the amount of NO released from these NO prodrugs is less than the expected quantities. It can be rationalized that for the trinitrosyl series (**11**, **12** and **13**) a very fast decomposition takes place generating only one peak implying that the release of all NO ligands occurs simultaneously, and that only part of the total amount of NO is detected. It is also known that NO can react at higher concentration with dissolved oxygen

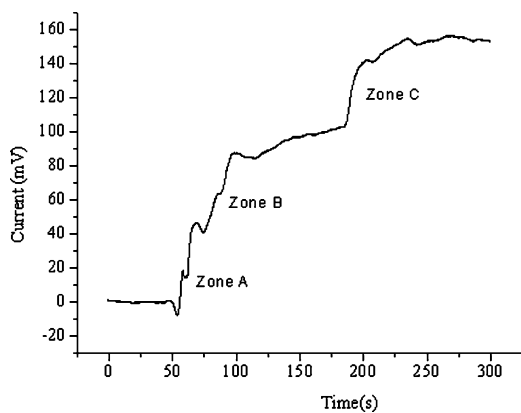


Fig. 11 Decomposition curve of $[\text{Fe}(\text{NO})_2\text{SCH}_2\text{CH}_2\text{NH}_3]_2\text{I}_2$ **6a** in water at 37°C .

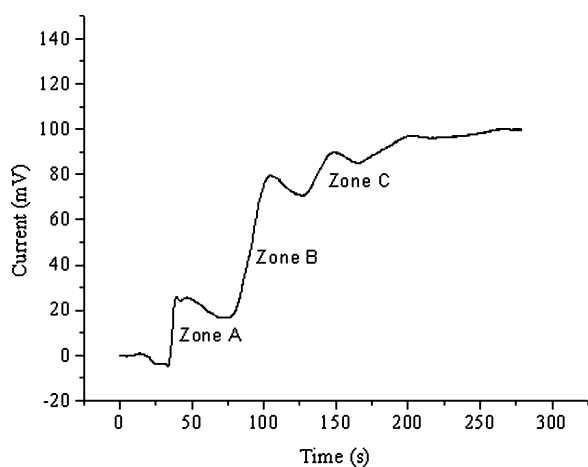


Fig. 12 Decomposition curve of $[\text{Fe}(\text{NO})_2\text{SCH}_2\text{CH}_2\text{NH}_3]_2\text{I}_2$ **6b** in water at 37°C .

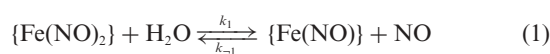
and water to give NO_x compounds as decomposition products, which can not be detected by the electrode.

For **6a** and **6b**, each step should correspond to the release of one NO molecule. The small amount of NO detected by the ISO-NO electrode could be explained by assuming that each free and detectable NO molecule is leaving the coordination sphere by replacement with a water molecule to give the hydrated species. However, if attack of a water molecule onto the still coordinated nitric oxide molecule occurs, other undetectable species such as HNO_2 are produced.

NO release kinetics: determination of the pseudo-first order rate constant of NO release from the NO donors using UV-vis spectroscopy

The most important factors of any NO prodrug are the equilibrium release and trapping amount of NO. The complexes to be studied were expected to possess bands in the UV-vis absorption region; it is then possible to determine the overall rate constant of NO release. The measurements were carried out under pseudo-physiological conditions (phosphate buffer $\text{pH} = 7.4$ and $T = 37^\circ\text{C}$) and concentrations in the millimolar range. The overall rate constant k_1 of the different NO donors was determined using pseudo-first-order conditions (eqn (1)). We assumed that

the equilibrium of NO release from these NO prodrugs can be described by the rate constants k_1 and k_{-1} of the pre-equilibrium.



The pseudo-first-order condition requires that the concentration of the reactant (here the NO prodrug) is at least 10 times smaller than that of all the other reactants (here the water). Plotting $\ln(A_0 - A_t)$ versus time gave in all cases a straight line.

Kinetics of the NO release of the nitric oxide donors. The high instability of the trinitrosyl series compounds **11**, **12** and **13** in water allowed kinetic studies³¹ only at room temperature in a phosphate buffer. These compounds exhibit bands in the UV-vis region at around 595 nm. **6a** and **6b** were also studied under the same pseudo-physiological conditions. The kinetics of the decomposition were established by monitoring the disappearance of the UV-vis band at 762 nm over time.³²

Based on a life time of approximately 100 s for **11**, **12** and **13**, and 300 s for **6a** and **6b**, the kinetic measurements of these compounds are not in accord with the results obtained by the electrochemical pathway. This can presumably be attributed to the fact that the disappearance of the UV-vis bands did not correspond to a process releasing NO, but to another, yet unidentified decomposition reaction. Therefore only the kinetic experiments of the nitroxyl donors can be taken with confidence in this section.

Kinetics of the NO^- release of the nitroxyl donors

$\text{Fe}(\text{NO})_2\text{P}(\text{CH}_2\text{OH})_3\text{Cl}$ **1** starts to release NO after an induction period of 10 min. The decomposition process is completed after 100 min. This process was followed by a decrease in the intensity of the band of **1** at around 520 nm. As demonstrated earlier in this paper this indicates the release of nitroxyl. A plot of the intensity of the absorption band at 520 nm permits the overall kinetics according to the $\ln(A_0 - A_t) = f(t)$ law to be established. The release of nitroxyl from **1** is slow and steady, while **2** decomposes in an incoherent way. It might be that the kinetics of the decomposition of **2** are more complex than the pseudo-first law would suggest. As a consequence, it was not possible to determine the rate constant k_1 of NO release for compound **2**. Finally $\text{Fe}(\text{NO})_2\text{HMPE}$ **4** compound was studied under the same conditions. The latter complex possesses a functionalised bisphosphine with high stability under pseudo-physiological conditions. **4** is completely stable even during an induction period of 260 min. After this it starts to decompose within 20 min (Table 5).

Conclusions

Water-soluble iron polynitrosyl complexes were prepared and tested for their potential application as NO donors. This became possible *via* their modification with water-soluble ligands such

Table 5 Values of rate constant k_1 of NO^- release for the nitroxyl donors **1** and **4** in phosphate buffer

Compounds	k_1/s^{-1}
$[\text{Fe}(\text{NO})_2\text{P}(\text{CH}_2\text{OH})_3\text{Cl}]$	3.71×10^{-4}
$[\text{Fe}(\text{NO})_2\text{HMPE}]$	1.35×10^{-5}

^a Experiments were performed at 37°C .

as functionalised phosphine, bisphosphine and sulfur containing molecules. Depending on the nature of the ligand, nitric oxide or nitroxyl donors were generated. Both compounds may be applicable for further *in vitro* and *in vivo* studies, because it has recently been suggested that nitric oxide and nitroxyl are both suitable substrates for the NOS (nitric oxide systems). The biophysical measurements using EPR and electrochemistry allowed us to identify and quantify the NO release from these prodrugs. Kinetic measurements carried out under pseudo-first order conditions allowed us to determine the pseudo-first order rate constant k_1 of the NO release under pseudo-physiological conditions. From all these experiments a step-wise mechanism of NO release is suggested.

Experimental

Material and methods

All reactions were carried out in an inert atmosphere using standard Schlenk-tube techniques or a dry-box (M. Braun 150 B-G). The solvents were dried using standard methods¹⁵ and stored under nitrogen prior to use. The deuterated solvents were also dried using standard methods and degassed using the “pump-thaw” method.

NMR spectra were recorded as follows: ¹H NMR: Bruker Avance DRX500, frequency 500.2 MHz and Varian Gemini 300, frequency 300.1 Hz; ¹³C{¹H} NMR: Bruker Avance DRX500, frequency 125.8 MHz and Varian Gemini 300, frequency 75.46 Hz; ¹⁹F NMR: Varian Gemini 300, frequency, 282.3 MHz; ³¹P NMR: Varian Gemini 300, frequency 121.5 MHz. Chemical shifts (δ) are given in ppm. If not otherwise mentioned, the spectra were recorded at room temperature. The references for the ¹H and ¹³C NMR spectra were the signals of the deuterated solvents (internal standard). For ¹⁹F NMR trifluorotoluene, and for ³¹P NMR spectra H₃PO₄ were used as an external standards. Some NMR spectra were also recorded using two-dimensional techniques (¹³C–¹H). IR spectra were recorded on a Bio-Rad FTS-45 Fourier IR spectrometer and low temperature IR spectra were measured using a Bio-Rad FTS-3500 Fourier IR spectrometer. UV-vis spectra were recorded on a Cary 500 scan UV-vis spectrometer. EPR spectra were recorded on a Bruker EMX-081 spectrometer between 245–255 K. EPR spectrometer settings were as follows, incident microwave power, 2 mW, modulation frequency, 100 kHz, frequency of 9.46 GHz, modulation amplitude, 10 G, and scan conditions (time constant, 2048 ms, sweep width, 700 G, sweep time, 167, 77 s); each spectrum was the result of signal of one scan. Conductivity was recorded with an Amel-160 conductimeter with Pt-cells. CHN-analyses were carried out using Leco CHNS-932 analyser.

The iron salts (FeSO₄·7H₂O, FeSO₄(NH₄)₂SO₄·6H₂O, FeCl₃·6H₂O, FeBr₂·4H₂O, Fe) were purchased from Fluka or Aldrich and used without further purification. The nitrosylating agents [NO][X] with X = BF₄, PF₆, SbF₆ were purchased from ABCR or Aldrich and used without further purification. NO gas (quality 2, Pangas, Suisse), for each experiment, was purified using a cold trap (pentane, liquid nitrogen, –90 °C) to remove all the impurities (N₂O₄, N₂O₃, NO₂).

Dinitrosyl(tris(hydroxymethyl)phosphine)chloroiron(II) 1. To a solution of the dimer [Fe(NO)₂Cl]₂ (0.100 g, 0.330 mmol) in 32 ml

toluene was added the tris(hydroxymethyl) phosphine (0.080 g, 0.645 mmol) dissolved in 6 ml of water. The mixture was stirred for 5 min and filtered off. The toluene phase was removed and the aqueous phase was evaporated under vacuum to give a red oil. This oil was washed with THF and recrystallized from ether. Yield: 70 mg (77%). IR (methanol): ν/cm^{-1} = 1720 (m, NO); 1678 (s, NO). ¹H NMR (water-d₂): δ 4.17 (s, 6H, CH₂OH). ¹³C NMR (water-d₂): δ 52.5 (d, ¹J = 75.8 Hz, CH₂OH). ³¹P NMR (water-d₂): δ 59.5 (s, PCH₂OH). Conductivity (H₂O): 195.56 S cm² mol⁻¹.

Dinitrosylbis(tris(hydroxymethyl)phosphine)iron(II) 2. To a solution of dicarbonyl dinitrosyliron (0.100 g, 0.582 mmol) in 40 ml of THF was added tris(hydroxymethyl)phosphine (0.130 g, 1.056 mmol). The solution was refluxed for 20 h. The red solution was filtered off and the solvent was removed under vacuum. Recrystallization from THF–ether gave **2**. Yield: 105 mg (50%). Found: C, 20.06; H, 4.71; N, 7.32%. C₆H₁₈FeN₂O₈P₂ required: C, 19.80; H, 4.94; N, 7.69%. IR (THF): ν/cm^{-1} = 1711 (m, NO); 1668 (s, NO). ¹H NMR (THF-d₈): δ 3.58 (s, 6H, CH₂); 4.56 (s, 3 H, OH). ³¹P NMR (THF-d₈): δ 52.1 (s, 2P). ¹³C NMR (THF-d₈): δ 59.3 (m, 3C, CH₂OH).

Dinitrosylbis(1,3,5-triaza-7-phosphatricyclo[3.3.1.1]decane)iron(II) 3. A solution of dicarbonyldinitrosyliron (0.100 g, 0.582 mmol) and 1,3,5-triaza-7-phosphatricyclo[3.3.1.1]decane (0.165 g, 0.105 mmol) in THF (40 ml) was refluxed for 16 h. The red solution was filtered off and the solvent removed under vacuum. Recrystallization from CH₂Cl₂–ether gave **3** as a light red compound. Yield: 75 mg (30%). Found: C, 32.24; H, 5.85. C₁₂H₂₄FeN₂O₈P₂ required: C, 32.52; H, 5.58. IR (THF): ν/cm^{-1} = 1715 (m, NO); 1668 (s, NO). ¹H NMR (THF-d₈): δ 4.05 (s, 6H, PCH₂N); 4.55 (s, 6H, NCH₂N). ¹³C NMR (THF-d₈): δ 56.1 (m, ¹J = 7 Hz, 3C, CH₂P); 73.6 (s, 3C, CH₂N). ³¹P NMR (THF-d₈): δ –25.5 (s).

Dinitrosyl(1,2-bis(dihydroxymethylphosphine)ethane)iron(II) 4. A solution of dicarbonyldinitrosyliron (0.100 g, 0.582 mmol) and HMPE (1,2-bis(dihydroxymethylphosphino)ethane) 0.125 g, 0.528 mmol) in 40 ml of THF was refluxed for 2 d. Removal of the solvent and recrystallization in THF–ether gave **4** as a red crystalline compound. Yield: 230 mg (74%). Found: C, 22.18; H, 4.86; N, 8.26%. C₁₂H₁₆FeN₂O₆ required: C, 21.85; H, 4.85; N, 8.49%. IR (THF): ν/cm^{-1} = 1711 (m, NO); 1664 (s, NO). ¹H NMR (THF-d₈): δ 1.98 (d, ²J = 16.5 Hz, 4H, PCH₂CH₂P); 4.0 (m, 8H, CH₂OH); 4.36 (m, 4H, OH). ³¹P NMR (THF-d₈): δ = 82.6 (s, 2P, PCH₂OH), ¹³C NMR (THF-d₈): δ 19.4 (dd, ¹J = ²J = 20 Hz, 2C, PCH₂CH₂P); 60.3 (m, 4C, CH₂OH).

Dinitrosyl(1,2-bis(dihydroxymethyl phosphine)benzene)iron(II) 5. 1,2-bis(dihydroxymethylphosphino)benzene (TMBz) (0.350 g, 1.63 mmol) was added to a solution of dicarbonyldinitrosyliron (0.280 g, 1.63 mmol) in 40 ml of THF. The mixture was refluxed during 40 h and then filtered off. Removal of the solvent under vacuum gave **5** as a brown powder. Yield: 246 mg (20%). Found: C, 32.17; H, 4.27; N, 7.15%. C₁₀H₁₆FeN₂O₆P₂ required: C, 31.78; H, 4.23; N, 7.41%. IR (THF): ν/cm^{-1} = 1715 (m, NO); 1666 (s, NO). ¹H NMR (THF-d₈): δ 4.20 (m, 12H, PCH₂OH); 7.5 (m, 4H, ArH). ³¹P NMR (THF-d₈): δ 76.0 (s, 2P). ¹³C NMR (THF-d₈): δ 61.5 (m, 4 C, PCH₂OH); 131.0 (s, 2C, ArC_{3,4}); 133.9 (t, ²J = 13 Hz, 2C, ArC_{2,5}); 145.0 (t, ¹J = 38 Hz, 2C, ArC_{1,6}).

Table 6 Crystal data for complexes 2, 3 and 4†

	2	3	4
Formula	C ₆ H ₁₈ FeN ₂ O ₈ P ₂	C ₁₆ H ₃₂ FeN ₈ O ₃ P ₂	C ₆ H ₁₆ FeN ₂ O ₆ P ₂
Molecular weight/g mol ⁻¹	364.01	502.29	330
Crystal description	Red, block	Red, plate	Red, block
Crystal size/mm	0.28 × 0.25 × 0.18	0.26 × 0.17 × 0.10	0.33 × 0.33 × 0.32
Crystal system	Triclinic	Monoclinic	Triclinic
Space group	<i>P</i> $\bar{1}$	<i>C</i> 2/ <i>c</i>	<i>P</i> $\bar{1}$
<i>a</i> /Å	6.8833(7)	19.4660(9)	7.6992(10)
<i>b</i> /Å	9.4457(9)	6.5409(4)	8.5741(11)
<i>c</i> /Å	11.4636(10)	19.0131(9)	11.2515(15)
<i>a</i> /°	89.368(11)	90	95.919(15)
<i>β</i> /°	72.801(11)	115.104(5)	106.994(15)
<i>γ</i> /°	77.584(11)	90	109.827(14)
<i>V</i> /Å ³	694.25(13)	2192.2(2)	651.11(18)
<i>Z</i>	2	4	2
<i>D_c</i> /g cm ⁻³	1.741	1.522	1.683
<i>T</i> /K	153	153	183
<i>λ</i> /Å	0.71073	0.71073	0.71073
<i>θ</i> range/°	2.97–30.27	3.32–30.28	2.87–30.39
Total no. of data	11 490	12 492	13 195
No. of unique data	3765	3253	3544
<i>F</i> (000)	376	1056	340
<i>R</i> ^{<i>ab</i>}	0.0496	0.0458	0.0268
<i>wR</i> ₂ ^{<i>ac</i>}	0.141	0.1215	0.0716
Observed data ^{<i>d</i>}	3064	2151	3022
Max., min. transmission	0.793, 0.704	0.918, 0.805	0.720, 0.601
Data/restraints/parameters	3765/0/178	3253/9/131	3544/0/164
Goodness-of-fit on <i>F</i> ²	1.091	0.912	1.078
Max., min. peaks/e Å ⁻³	2.13, -1.30	0.892, -0.728	0.558, -0.694

^a Observation criteria $I > 2\sigma(I)$. ^b $R = \sum \|F_o\| - |F_c| / \sum \|F_o\|$. ^c $wR_2 = \{\sum [w(F_o^2 - F_c^2)^2] / \sum [w(F_o^2)^2]\}^{1/2}$.

Table 7 Crystal data for complexes 6b, 9, 10 and 11†

	6b	9	10	11
Formula	C ₄ H ₁₄ Fe ₂ I ₂ N ₆ O ₅ S ₂	C ₈ H ₈ Fe ₂ N ₈ O ₄ S ₂	C ₈ H ₁₄ FeIN ₄ O ₅ S	C ₃ H ₅ F ₆ FeN ₅ O ₆ P ₂
Molecular weight/g mol ⁻¹	659.88	465.06	429.05	414.92
Description	Red, plate	Red opaque, block	Red opaque, block	Green, tiny plate
Crystal size/mm	0.32 × 0.20 × 0.09	0.31 × 0.24 × 0.19	0.26 × 0.14 × 0.10	(Irregular shape)
Crystal system	Triclinic	Triclinic	Monoclinic	Orthorhombic
Space group	<i>P</i> $\bar{1}$	<i>P</i> $\bar{1}$	<i>P</i> 2 ₁ / <i>n</i>	<i>Pna</i> 2 ₁
<i>a</i> /Å	6.3097(5)	6.4219(13)	7.0648(4)	24.693(3)
<i>b</i> /Å	6.8752(5)	7.626(2)	11.4932(7)	6.6317(10)
<i>c</i> /Å	24.5366(17)	8.345(2)	18.8432(10)	8.2556(16)
<i>a</i> /°	90.403(8)	75.61(3)	90	90
<i>β</i> /°	93.515(8)	80.83(3)	91.237(7)	90
<i>γ</i> /°	116.319(8)	85.15(3)	90	90
<i>V</i> /Å ³	951.58(14)	390.37(17)	1529.66(15)	1351.9(4)
<i>Z</i>	2	1	4	4
<i>D_c</i> /g cm ⁻³	2.303	1.940	1.863	2.039
<i>T</i> /K	153	183	153	183
<i>λ</i> /Å	0.71073	0.71073	0.71073	0.71073
<i>θ</i> range/°	2.50–28.02	3.28–30.33	2.80–30.31	3.18–30.52
Total no. of data	10 041	6823	17 573	6204
No. of unique data	4195	2102	4499	2046
<i>F</i> (000)	628	228	836	824
<i>R</i> ^{<i>ab</i>}	0.0283	0.0319	0.0479	0.0949
<i>wR</i> ₂ ^{<i>ac</i>}	0.0767	0.1066	0.1252	0.2201
Observed data ^{<i>d</i>}	3491	1752	2709	1023
Max., min. transmission	0.661, 0.297	0.685, 0.554	0.744, 0.495	—, —
Data/restraints/parameters	4195/0/194	2102/0/109	4499/0/166	2046/23/199
Goodness-of-fit on <i>F</i> ²	1.009	1.090	1.005	1.234
Max., min. peaks/e Å ⁻³	1.5, -1.582	0.550, -1.091	2.080, -1.752	0.961, -0.990

^a Observation criteria $I > 2\sigma(I)$. ^b $R = \sum \|F_o\| - |F_c| / \sum \|F_o\|$. ^c $wR_2 = \{\sum [w(F_o^2 - F_c^2)^2] / \sum [w(F_o^2)^2]\}^{1/2}$.

Di- μ -cysteaminehydrochloridetetranitrosyldiiron(I) 6a. To a solution of dicarbonyldinitrosyliron (0.100 g, 0.582 mmol) in 30 ml of THF was added cysteamine hydrochloride (0.066 g, 0.582 mmol). The mixture was refluxed overnight and the precipitate was filtered off and dried under vacuum to give **6** as an ochre precipitate. Yield: 11 mg (40%). Found: C, 13.14; H, 3.02; N, 17.05%. $C_4H_{14}Cl_2Fe_2N_6O_4S_2$, $S(CH_2)_2NH_3Cl$ required: C, 12.66; H, 3.68; N, 17.21%. IR (Nujol): $\nu/cm^{-1} = 1754$ (m, NO); 1753 (s, NO). 1H NMR (water- d_2): δ 1.77 (s, 2H, CH_2S); 3.4 (m, 2H, CH_2NH_3Cl). ^{13}C NMR (water- d_2): δ 22.8 (s, 2H, SCH_2); 65.7 (s, 2H, CH_2NH_3Cl).

Di- μ -cysteaminehydroiodidetetranitrosyldiiron(I) 6b. A mixture of di- μ -iodotetranitrosyldiiron $[Fe(NO)_2I]_2$ (0.100 g, 0.205 mmol) and cysteine (0.016 g, 0.205 mmol) in 20 ml of THF was stirred at room temperature for 18 h. The brown precipitate was filtered off and washed several times with ether and dried under vacuum to give **7**. Yield: 124 mg (95%). Found: C, 12.63; H, 2.97; N, 12.06%. $C_4H_{14}I_2Fe_2N_6O_4S_2$, required: C, 13.53; H, 2.81; N, 11.83%. IR (Nujol): $\nu/cm^{-1} = 1782$ (s, NO); 1715 (s, NO); 1464 (m, NH_3). 1H NMR (water- d_2): δ 3.3 (m, 4H, CH_2CH_2). ^{13}C NMR (water- d_2): δ 37.9 (d, $^1J = 8$ Hz, SCH_2); 39.5 (d, $^1J = 4$ Hz, CH_2NH_2).

Di- μ -cysteineethanoatetetranitrosyldiiron(I) 8. To a solution of dicarbonyldinitrosyliron (0.100 g, 0.582 mmol) in 40 ml of THF the L-cysteine ethyl ester hydrochloride (0.307 g, 0.582 mmol) was added. The mixture was stirred at room temperature for 3 d. The solution was evaporated under vacuum to give **8** as a deep green product. Yield: 181 mg (81%). Found: C, 23.00; H, 4.02. $C_{10}H_{20}Fe_2N_6O_8S_2$ required: C, 22.66; H, 4.15. IR (Nujol): $\nu/cm^{-1} = 1755$ (m, NO); 1711 (s, $CO(O)Et$); 1595 (w, NH_2). 1H NMR (THF- d_8): δ 0.88 (m, 2H, CH_2CH_3); 1.35 (m, 3H, CH_2CH_3); 4.39 (m, 3H, CH_2CH). ^{13}C NMR (THF- d_8): δ 14.2 (s, $S-CH_2$); 23.1 (s, NH_2CH); 26.3 (s, OCH_2CH_3); 34.9 (s, OCH_2CH_3); 64.1 (s, $CO(OCH_2CH_3)$).

Di- μ -(pyrimidine-2-thionate)tetranitrosyldiiron(I) 9. To a solution of dicarbonyldinitrosyliron (0.100 g, 0.582 mmol) in 40 ml of THF was added pyrimidine-2-thiol (0.065 g, 0.582 mmol). The solution is refluxed for 16 h. Removal of the solvent under vacuum gave **9** as a black solid. Yield: 132 mg (50%). Found: C, 21.36; H, 1.40; N, 24.40%. $C_8H_6Fe_2N_8O_4S_2$ requires: C, 21.07; H, 1.75; N, 24.57%. IR (THF): $\nu/cm^{-1} = 1794$ (m, NO); 1759 (s, NO). 1H NMR (THF- d_8): δ 7.14 (s, 1H, CH_{pyr}); 8.55 (s, 2H, $2CNCH_{pyr}$). ^{13}C NMR (THF- d_8): δ 121.0 (s, $C_{pyr}HCH$); 158.5 (s, $2C_{pyr}N$); 174.0 (s, $C_{pyr}S$).

Dinitrosyl(pyrimidine-2-thionate)iiodoiron(0) 10. A solution of $[Fe(NO)_2I]_2$ (0.100 g, 0.205 mmol) and pyrimidine-2-thiol (0.023 g, 0.205 mmol) in 40 ml of THF was stirred for 3 h at room temperature. Recrystallization from THF-ether gave **10** as a black solid. Yield: 79 mg (67%). Found: C, 18.44; H, 2.10; N, 14.32%. $C_8H_6IFe_2N_8O_4S_2$ required: C, 18.39; H, 2.29; N, 14.29%. IR (THF): $\nu/cm^{-1} = 1790$ (m, NO); 1722 (s, NO). 1H NMR (THF- d_8): δ 3.4 (m, 1H, $H_{pyr}CH$); 3.58 (s, 2H, $H_{pyr}CHN$). ^{13}C NMR (THF- d_8): δ 15.6 (s, $2C$, CHN); 66.3 (s, $2C$, CH_2 ; $C-S$).

Trinitrosyl(tris(hydroxymethyl)phosphine)iron(II) hexafluorophosphate 11. To a solution of dicarbonyldinitrosyliron (0.050 g, 0.290 mmol) in 3 ml of nitromethane at $-30^\circ C$ was added NOPF₆ (0.050 g, 0.290 mmol) in small portions.

The solution changed from red to green. Then a solution of trishydroxymethylphosphine (0.036 g, 0.290 mmol) in 3 ml of nitromethane was added dropwise. To precipitate **11**, a large portion (20 ml) of cold toluene was added. The green product was filtered off and dried under vacuum. Due to the instability of **11** at room temperature a correct elemental analysis could not be obtained. Yield: 85 mg (63%). IR (nitromethane, $-10^\circ C$, CaF_2): $\nu/cm^{-1} = 1927$ (w, NO); 1833 (vs, NO). 1H NMR (nitromethane- d_3): δ 4.73 (s, 6H, CH_2OH). ^{13}C NMR (nitromethane- d_3): δ 55.0 (d, $^1J = 50$ Hz, CH_2OH). ^{19}F NMR (nitromethane- d_3): δ -72.0 (d, $^1J = 714$ Hz, 6F, PF_6). ^{31}P NMR (nitromethane- d_3): δ -144.0 (hept., $^1J = 715$ Hz, PF_6); 46.0 (s, $P(CH_2OH)_3$).

Trinitrosyl(tris(hydroxymethyl)phosphine)iron(II) tetrafluoroborate 12. The same procedure as for **11** was used to synthesise the trinitrosyl(trishydroxymethylphosphine)iron(II) tetrafluoroborate **12**, and the hexafluoroantimonate **13**, using nitrosoniumtetrafluoroborate for **12** and nitrosoniumhexafluoroantimonate for **13** as nitrosylating agents. Due to the instability of **12** at room temperature a correct elemental analysis could not be obtained. Yield: 74 mg (63%). IR (nitromethane, $-10^\circ C$, CaF_2): $\nu/cm^{-1} = 1927$ (w, NO); 1835 (vs, NO). 1H NMR (nitromethane- d_3): δ 4.79 (s, 6H, CH_2OH). ^{13}C NMR (nitromethane- d_3): δ 57.0 (sb, CH_2OH). ^{31}P NMR (nitromethane- d_3): δ 47.0 (s, $P(CH_2OH)_3$). ^{19}F NMR (nitromethane- d_3): δ -144.0 (s, BF_4).

Trinitrosyl(tris(hydroxymethyl)phosphine)iron(II) hexafluoroantimonate 13. Due to the instability of **13** at room temperature a correct elemental analysis could not be obtained. Yield: 34 mg (21%). IR (nitromethane, $-10^\circ C$, CaF_2): $\nu/cm^{-1} = 1927$ (w, NO); 1835 (s, NO). 1H NMR (nitromethane- d_3): δ 4.82 (s, 6H, CH_2OH). ^{31}P NMR (nitromethane- d_3): δ 46.0 (s, $P(CH_2OH)_3$). ^{13}C NMR (nitromethane- d_3): δ 57.5.

Crystal data are given in Tables 6 and 7.

CCDC reference numbers 610298–610305.

For crystallographic data in CIF or other electronic format see DOI: 10.1039/b702461d

References

- 1 A. R. F. Furchgott and J. V. Zawadzki, *Nature*, 1980, **288**, 373–376; S. Moncada, R. M. J. Palmer and E. A. Higgs, *Pharm. Rev.*, 1991, **43**, 109–141; R. F. Furchgott, *Vasodilation: Vascular Smooth Muscle, Peptides, and Endothelium*, ed. P. M. Vanhoutte, Raven Press, New York, 1988, pp. 401–414; S. Moncada, R. M. J. Palmer and E. A. Higgs, *Pharm. Rev.*, 1991, **43**, 109–141; N. Miki, Y. Kawabe and K. Kuriyama, *Biochem. Biophys. Res. Commun.*, 1977, **75**(4), 851–856.
- 2 R. F. Furchgott and J. V. Zawadzki, *Nature*, 1980, **288**, 373–376.
- 3 F. Murad, *Angew. Chem., Int. Ed.*, 1999, **38**, 1856–1868; R. F. Furchgott, *Angew. Chem., Int. Ed.*, 1999, **38**, 1870–1880; L.-J. Ignarro, *Angew. Chem., Int. Ed.*, 1999, **38**, 1882–1892.
- 4 A. R. Butler and C. Glidewell, *Chem. Soc. Rev.*, 1987, **16**, 361–380; E. A. Kowaluk, P. Seth and H.-L. Fung, *J. Pharmacol. Exp. Ther.*, 1992, **262**(3), 916–922.
- 5 P. G. Wang, M. Xian, X. Tang, X. Wu, Z. Wen, T. Cai and A. J. Janczuk, *Chem. Rev.*, 2002, **102**, 1091–1134.
- 6 D. J. Stuehr, S. S. Gross, I. Sakuma, R. Levi and C. F. Nathan, *J. Exp. Med.*, 1989, **169**, 1011–1020; Pellat, Y. Henry and J.-C. Drapier, *Nitric oxide from L-arginine: a bioregulatory system*, ed. S. Moncada and E. A. Higgs, Elsevier, Amsterdam, 1990, pp. 281–289.
- 7 M. E. Murphy and H. Sies, *Proc. Natl. Acad. Sci. USA*, 1991, **88**, 10860–10864.
- 8 K. Shibuki, *Neurosci. Res.*, 1990, **9**, 69–76; T. Malinski and Z. Taha, *Nature*, 1992, **358**, 676–8.

- 9 F. L. Atkinson, H. E. Blackwell, N. C. Brown, N. G. Connelly, J. G. Crossley, A. G. Orpen, A. L. Rieger and P. H. Rieger, *J. Chem. Soc., Dalton Trans.*, 1996, 3491–3502.
- 10 D. Ballivet-Tkatchenko and C. Billard, *J. Polym. Sci., Polym. Chem. Ed.*, 1981, **19**, 1697–1706.
- 11 J. W. Ellis, K. N. Harrison, P. A. T. Hoye, A. G. Orpen, P. G. Pringle and M. B. Smith, *Inorg. Chem.*, 1992, **31**, 3026–3033.
- 12 D. W. McBride, S. L. Stafford and G. A. Stone, *Inorg. Chem.*, 1962, **1**(2), 386–388.
- 13 L. Malatesta and A. Araneo, *J. Chem. Soc.*, 1957, 3803–3805; V. G. Albano, A. Araneo, P. L. Bellon, G. Ciani and M. Manassero, *J. Org. Chem.*, 1974, **67**, 413–422.
- 14 J. T. Lin, S. Y. Wang, Y. C. Chou, M. L. Gong, Y.-M. Shioh, H.-M. Gau and Y. S. Wen, *J. Org. Chem.*, 1996, **508**, 183–193.
- 15 J. W. Ellis, K. N. Harrison, P. A. T. Hoye, A. G. Orpen, P. G. Pringle and M. B. Smith, *Inorg. Chem.*, 1992, **31**, 3026–3033; V. G. Albano, A. Araneo, P. L. Bellon, G. Ciani and M. Manassero, *J. Org. Chem.*, 1974, **67**, 413–422.
- 16 D. J. Daigle, T. J. Decuir, J. B. Robertson and D. J. Darensbourg, Ligands for Water-Solubilizing Org. Com., *Inorg. Synth.*, ed. M. Y. Darensbourg, John Wiley & Sons Inc., New York, 1998, 40–44; M. Y. Darensbourg and D. Daigle, *Inorg. Chem.*, 1975, **14**(5), 1217–1218.
- 17 V. G. Albano, A. Araneo, P. L. Bellon, G. Ciani and M. Manassero, *J. Org. Chem.*, 1974, **67**, 413–422.
- 18 V. S. Reddy, D. E. Berning, K. V. Katti, C. L. Barnes, W. Y. Volkert and A. R. Ketrang, *Inorg. Chem.*, 1996, **35**, 1753–1757.
- 19 (a) R. E. Rundle, *J. Phys. Chem.*, 1957, **61**, 45–50; R. V. G. Evens, *Nature*, 1948, **161**, 530–531; P. S. Braterman, V. A. Wilson and K. K. Joshi, *J. Chem. Soc. A*, 1971, 191–195; (b) W. E. Douglas and M. L. H. Green, *J. Chem. Soc., Dalton Trans.*, 1972, 1796–1800.
- 20 K. A. Jensen, *Z. Anorg. Allg. Chem.*, 1936, **229**, 265–281; D. C. Jicha and D. H. Busch, *Inorg. Chem.*, 1962, **1**(4), 872–877; D. C. Jicha and D. H. Busch, *Inorg. Chem.*, 1962, **1**(4), 878–883; D. H. Busch and D. C. Jicha, *Inorg. Chem.*, 1962, **1**(4), 884–886; T. Yonemura, Z.-P. Bai, K.-I. Okamoto, T. Ama, H. Kawaguchi, T. Yasui and J. Hidaka, *J. Chem. Soc., Dalton Trans.*, 1999, 2151–2157.
- 21 H. Soling and R. W. Asmussen, *Acta Chem. Scand.*, 1957, **11**, 1534–1540; B. Haymore and R. D. Feltham, *Inorg. Synth.*, 1973, **XIV**, 81–92; T. Moeller and D. H. Wilkins, *Inorg. Synth.*, 1953, **IV**, 101–103; S. Y. Tyree, *Inorg. Synth.*, 1953, **IV**, 104–111; W. Hieber and R. Marin, *Z. Anorg. Allg. Chem.*, 1939, **240**, 241–260; W. Hieber and J. S. Anderson, *Z. Anorg. Allg. Chem.*, 1933, **211**, 132–140.
- 22 K. Yamanari, K. Okusako and S. Kaizaki, *J. Chem. Soc., Dalton Trans.*, 1992, 1615–1619; K. Yamanari, K. Okusako, Y. Kushi and S. Kaizaki, *J. Chem. Soc., Dalton Trans.*, 1992, 1621–1626; D. L. Geffner, M. Azukizawa and J. M. Hershman, *J. Clin. Invest.*, 1975, **75**, 224–229.
- 23 W. Hieber and K. Kaiser, *Z. Anorg. Allg. Chem.*, 1968, **358**, 271–281. 49; V. M. Kothari and D. H. Busch, *Inorg. Chem.*, 1969, **8**(11), 2276–2280; C. P. Sloan and J. H. Krueger, *Inorg. Chem.*, 1975, **14**(7), 1481–1485; H. C. Freeman, C. J. Moore, W. G. Jackson and A. M. Sargeson, *Inorg. Chem.*, 1978, **17**(12), 3513–3521.
- 24 F. Seel, *Z. Anorg. Allg. Chem.*, 1942, **249**, 309–324.
- 25 M. T. Mocella, M. S. Okamoto and E. K. Barefield, *Synth. React. Inorg. Met.-Org. Chem.*, 1974, **4**(1), 69–90.
- 26 M. N. Hughes and R. Camack, *Methods Enzymol.*, 1999, **301**, 279–281; Y. Xia, A. J. Cardounel, A. F. Vanin and J. L. Zweier, *Free Radical Biol. Med.*, 2000, **29**(8), 793–797.
- 27 L. A. Shinobu, S. G. Jones and M. M. Jones, *Acta Pharmacol. Toxicol.*, 1984, **54**, 189–194.
- 28 M. N. Hughes and R. Camack, *Methods Enzymol.*, 1999, **301**, 279–281.
- 29 M. Feelisch and J. S. Stamler, *Methods in Nitric Oxide Research*, John Wiley & Sons Inc., New York, 1996.
- 30 *ISO-NO Mark II Instruction Manual*, World Precision Instruments, Inc., Sarasota, FL, USA, 2002.
- 31 T. Yonemura, S. Nakahira, T. Ama, H. Kawaguchi, T. Yasui, K.-I. Okamoto and J. Hidaka, *Bull. Chem. Soc. Jpn.*, 1995, **68**, 2859–2866; S.-I. Aizawa, K.-I. Okamoto, H. Einaga and J. Hidaka, *Bull. Chem. Soc. Jpn.*, 1988, **61**, 1601–1606; K.-I. Okamoto, T. Yonemura, T. Konno and J. Hidaka, *Bull. Chem. Soc. Jpn.*, 1992, **65**, 794–798.
- 32 R. B. Jordan, *Reaction Mechanism of Inorg. and Org. Systems*, Oxford University Press, Oxford, 1998; H.-H. Perkampus, *UV-Vis-Spektroskopie und ihre Anwendungen*, Springer-Verlag, Berlin, 1986.